

ORIGINAL RESEARCH PAPER

Wavelet method optimised by ant colony algorithm used for extracting stable and unstable signals in intelligent substations

Tianyan Jiang^{1,2} | Xiao Yang¹  | Yuan Yang¹  | Xi Chen¹ | Maoqiang Bi¹ | Jianfei Chen³

¹School of Electrical and Electronic Engineering, Chongqing University of Technology, Chongqing, China

²Department State Key Laboratory of Power Transmission Equipment & System and New Technology, Chongqing University, Chongqing, China

³Department of Electrical and Computer Engineering, University of Maryland, College Park, Maryland, USA

Correspondence

Maoqiang Bi, School of Electrical and Electronic Engineering, Chongqing University of Technology, Chongqing, China.

Email: bimaqiang@cqut.edu.cn

Funding information

Program of Chongqing Banan District, Grant/Award Number: 2020QC407; Chongqing Municipal Education Commission, Grant/Award Number: KJQN202001146; National Key Research and Development Program, Grant/Award Number: 2018YFB2100100; Joint Funds of the National Natural Science Foundation of China, Grant/Award Number: U1866603

Abstract

Partial discharge (PD) signals are an important index to evaluate the operation state of intelligent substations. The correct distinction of PD pulse and interference pulse has become a challenging task. Because of the noise and the low signal-to-noise ratio, the stable signals become non-stationary. The selection of a wavelet basis, the selection rule of threshold λ and the design of the threshold function are the key factors affecting the final denoising effect. Therefore, an enhanced ant colony optimisation wavelet (ACOW) algorithm was applied to find the global optimal threshold through the continuous derivative threshold function and the ant colony optimisation (ACO) algorithm. At the same time the efficiency of adaptive search calculation, was also significantly improved. The method of the ACOW algorithm was compared with the soft wavelet method, gradient-based wavelet method and the genetic optimisation wavelet (GOW) method. Using these four methods to denoise four typical signals, different mean square errors (MSE), magnitude errors (ME) and time costs were obtained. Interestingly, the results show that the ACOW method can achieve the minimum MSE and has less time cost. It generates significantly smaller waveform distortion than the other three threshold estimation methods. In addition, the high efficiency and good quality of the output signals are beneficial to the diagnosis of local discharge signals in intelligent substations.

1 | INTRODUCTION

For meeting the demand of substation automation communication system standards, realising rapid and accurate detection and transmission of signals, the PD signals detected by power equipment must be digitally transmitted [1, 2]. Because of the strong electromagnetic waves, these signals must be denoised using certain digital approaches before being transferred [3]. Condition signals, including stable signals like voltage and current signals, are used for relay protection. And unstable signals like partial discharge (PD) signals are vital for evaluating

the conditions of electrical equipment [4]. The way of the wavelet method is widely used in intelligent substations for denoising PD signals. It is vital for avoiding electrical accidents from happening or reducing them to extract discharge information. Therefore, denoise signals play an important role in the processing of PD signals [5–7].

Obtaining the minimum mean squared error (MSE) and the best wavelet parameters is the key work of denoising signals. Recently, for solving the issue of denoising signals, various optimisation algorithms have been proposed in different fields, for example, clinical diagnosis, PD, and so on. Z.A.A. Alyasseri

This is an open access article under the terms of the Creative Commons Attribution License, which permits use, distribution and reproduction in any medium, provided the original work is properly cited.

© 2021 The Authors. *CAAI Transactions on Intelligence Technology* published by John Wiley & Sons Ltd on behalf of The Institution of Engineering and Technology and Chongqing University of Technology.

et al. in [8–12] proposed the hybridising method that involves the wavelet transform with the β -Hill climbing algorithm and the wavelet transform with the genetic algorithm, which were used for denoising electrocardiogram (ECG) and the electroencephalogram (EEG) signals by obtaining the optimal wavelet parameters. The proposed method had high efficacy and reliability. The literature [13] presents db4, sym7, bior3.9, and coif3, which are four mother wavelet functions, to denoise EEG signals.

Obtaining the global optimal threshold and improving the convergence accuracy and speed are challenge tasks. Different advanced optimisation algorithms have been proposed by many scholars. Cai et al. [14] showed a method involving an improved quantum-inspired cooperative co-evolution algorithm to improve the global search capability. Deng et al. [15, 16] came up with an improved differential evolution algorithm with a wavelet basis function to obtain better optimisation capabilities and higher convergence accuracy. Y.J. Song et al. [17] had an enhanced success history when they used calculate-adaptive DE for parameter optimisation of photovoltaic models. Deng et al. [18] presented an improved PSO-based QEA method to calculate gate resource allocation. Deng et al. [19] have solved the global optimisation problems using an enhanced improved quantum-inspired differential evolution with multistrategies algorithm with novel multiple strategies. Studies [20] show the calculation of the optimal threshold of the wavelet shrinkage method by the gradient-based wavelet (GW) threshold. However, it shows the disadvantages of denoising PD signals, as demonstrated in the literature [21]. The genetic approach [22] is used to denoise PD signals and its procedure is explained in [23, 24]. However, the genetic procedure is complicated and following it to extract the signals in the field is time consuming [25–27]. The aim of the article is to get a faster and more robust method for denoising the state signals of smart substations [28–30].

Because of the robustness, stability, and high efficiency of the wavelet method, and the robustness and quick convergence of the ant colony optimisation (ACO) algorithm, an enhanced wavelet method, improved by the ACO algorithm, is applied to extract the stable and unstable signals in intelligent substations and this method has been presented in this article. In the ant colony optimisation wavelet (ACOW), the continuous derivative threshold function and the ACO algorithm is used to obtain the global optimal threshold. The efficiency of the adaptive search calculation is also significantly improved. The ACOW is used to estimate the threshold value of wavelet and denoise signals. The soft wavelet (SW) method, GW method and the genetic optimisation wavelet (GOW) method are also used for denoising comparative experiments. The results demonstrate that the ACOW method can effectively clear white noise. Compared with the other three algorithms, the ACOW shows a superior denoising ability.

The main contributions of the article are showed as follows:

- (1) An enhanced wavelet method improved by the ACO algorithm is used to effectively clear white noise. Based

on the continuous derivative threshold function and the ACO algorithm, the global optimal threshold can be obtained.

- (2) The ACOW causes a significantly smaller distortion to denoised signals than any of the other methods. In addition, compared with other methods, it has a faster calculation speed and is more robust.
- (3) Among all the other methods, the ACOW method can achieve the minimum mean square error (MSE) and magnitude error (ME).

The remaining part of the article is arranged as follows: Section 2 illustrates the types of stable and unstable signals and how to establish them. Section 3 introduces the ant colony optimisation (ACO) wavelet method in detail. Section 4 shows the denoising experiment and analyses the experimental results of four methods. The conclusion is presented in Section 5.

2 | CONDITION SIGNALS IN INTELLIGENT SUBSTATIONS

Quite a few stable signals exist in intelligent substations, for example, stable voltage and current signals' output by transformers. But the influence of harmonics and electromagnetic interference make the stable signals distorted. Therefore, Blocks, Bumps, HeaviSine and Doppler signals [19], with lengths of 4096 points, are selected to simulate the stable voltage and current signals with harmonics in intelligent substations, as illustrated in Figure 1.

There are some non-stable signals in intelligent substations, among which the PD signals are one of the typical short-term transient signals. And the signals that the PD online monitoring broadband measurement system may measure can be simulated by the attenuation oscillation pulse s , which is shown (1) in the following:

$$s(t) = M[e^{-\alpha_1 t} \cos(\omega t - \psi) - e^{-\alpha_2 t} \cos(\psi)] \quad (1)$$

where M is the amplitude coefficient, α_1 and α_2 are attenuation constants, $\omega = 2\pi f$ is the oscillation frequency and $\psi = \arctan(\omega/\tau_2)$.

Figure 2 shows two simulative PD high-frequency signals with lengths of 2048 points used to simulate the non-stable condition signals. The parameters of vibrate PD signals in this article are $M = 1$, $\alpha_1 = \times 10^6 \text{ s}^{-1}$, $\alpha_2 = 1 \times 10^7 \text{ s}^{-1}$, $f = 1 \text{ MHz}$, as illustrated in Figure 2(b).

We not only compare with the denoising effect of different kinds of simulative signals but also the field PD signal. Figure 3 shows a field PD signal detected in a 500 kV electrical transformer by a PD online monitoring system. The system includes a sampling system, with a sampling rate of 3mb/s, and a high-frequency current transformer, with a frequency passband between 50 kHz and 1 MHz.

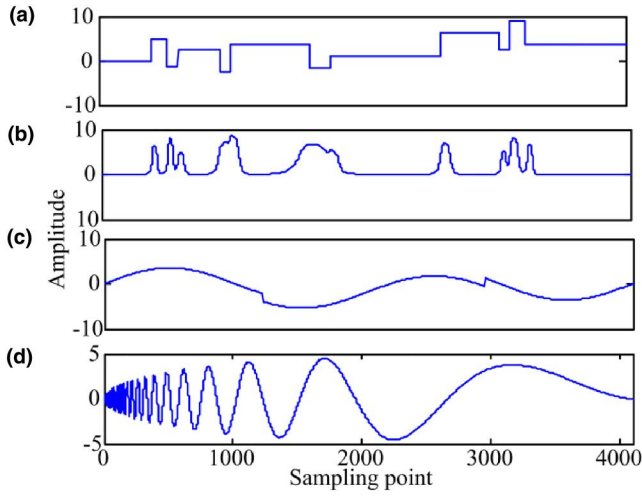


FIGURE 1 Four artificially stable signals. (a)–(d) signals of Blocks, Bumps, HeaviSine and Doppler

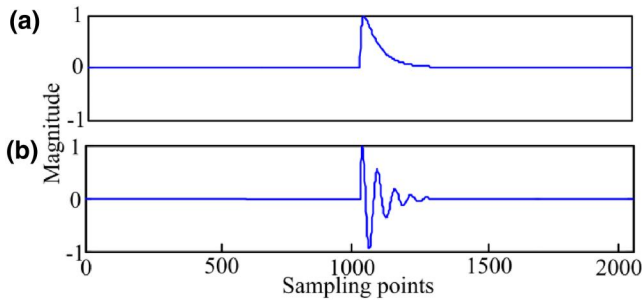


FIGURE 2 Simulative partial discharge (PD) high-frequency signals. (a) pulse partial discharge signal; (b) vibrating partial discharge signal

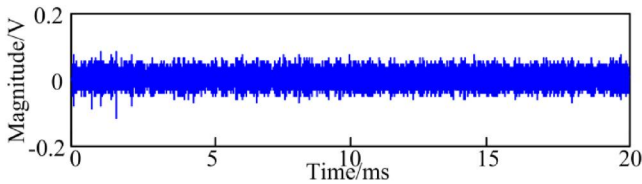


FIGURE 3 Detected partial discharge high-frequency signal

3 | ANT COLONY Optimisation WAVELET METHOD

At moment i , suppose sequence $Y = \{y_1, y_2, \dots, y_{N-1}\}$ is an observation of the noise signals and sequence $s = \{s_0, s_1, \dots, s_{N-1}\}$ is the true value of the signals.

$$y_i = s_i + n_i \quad i = 0, 1, 2, \dots, N-1 \quad (2)$$

where n_i is a separate distribution of Gaussian white noise. The estimated signal \hat{S} of noise signal Y can be derived by wavelet denoising and make the minimum MSE of both \hat{S} and s .

The threshold $\lambda(t+1)$ for the number of iterations of $t-1$ equals to the threshold $\lambda(t)$ for the number of iterations of t minus the MSE $\xi(t)$ function gradient values $\Delta\lambda(t)$, as follows:

$$\lambda(t+1) = \lambda(t) - \mu\Delta\lambda(t) \quad (3)$$

where μ is step [31] and $\Delta\lambda(t)$ is expressed as Equation (4).

$$\Delta\lambda(t) = 2 \sum_k g_k \frac{\partial \eta(d_{j,k}, \lambda)}{\partial \lambda} + 2 \sum_k \frac{\partial^2 \eta(d_{j,k}, \lambda)}{\partial \lambda \partial d_{j,k}} \quad (4)$$

where g_k is the function estimate expression and $d_{j,k}$ is the wavelet detail coefficient of scale j .

In Equation (4), the hard threshold function and soft threshold function cannot perform adaptive iterations because of their discontinuous derivatives. Therefore, the best threshold cannot be obtained.

For obtaining the best threshold, another threshold function is presented in this article as Equation (5).

$$\eta_\alpha(y, \lambda) = \begin{cases} y - \alpha \cdot \lambda^2 / y & |y| > \lambda \\ \alpha \cdot y^3 & |y| \leq \lambda \end{cases} \quad (5)$$

where α is a real number and $\alpha = 0.5$ in this article.

Equations (6) and (7) represent the first derivative and the second-order derivative, respectively, of the hard threshold function, soft threshold function and $\eta_\alpha(y, \lambda)$, as follows:

$$\frac{\partial \eta_\alpha(d_{j,k}, \lambda)}{\partial \lambda} = \begin{cases} -2\alpha \cdot \lambda / d_{j,k} & |d_{j,k}| > \lambda \\ -2\alpha \cdot d_{j,k}^3 / \lambda^3 & |d_{j,k}| \leq \lambda \end{cases} \quad (6)$$

$$\frac{\partial^2 \eta_\alpha(d_{j,k}, \lambda)}{\partial \lambda \partial d_{j,k}} = \begin{cases} -2\alpha \cdot \lambda / d_{j,k}^2 & |d_{j,k}| > \lambda \\ -6\alpha \cdot d_{j,k}^2 / \lambda^3 & |d_{j,k}| \leq \lambda \end{cases} \quad (7)$$

By replacing (3) and (4) with types 5, 6 and 7, the adaptive iteration calculation of the wavelet thresholds can be carried out and the optimal wavelet threshold can be obtained.

The ACO algorithm has many advantages. It is a simple and robust algorithm with few parameters and is suitable for field applications. Therefore, we use the ant colony algorithm to improve the GW method, the procedure of which is presented in [19, 23].

Multi-scale wavelet coefficients of condition signals are calculated by wavelet decomposition. Threshold λ in the GW method, randomly obtained between λ_{\min} and λ_{\max} , is each ant in the ACOW. The calculated equations of λ_{\min} and λ_{\max} , described in the literature [23], are adopted in this article. The evaluation of the fitness of each individual ant is denoted by $\Delta\lambda(n)$, as expressed in Equation (8) [19]. When it reaches the minimum value, the optimum threshold is obtained.

$$\Delta\lambda(n) = 2 \sum_k g_k \frac{\partial \eta(d_{j,k}, \lambda)}{\partial \lambda} + 2 \sum_k \frac{\partial^2 \eta(d_{j,k}, \lambda)}{\partial \lambda \partial d_{j,k}} \quad (8)$$

where the threshold function $\eta(d_{j,k}, \lambda)$, used in this manuscript, is referred, as in [25].

The probability $P_{p,q}^k(n)$ of the k th ant moving from city p to city q is shown in Equation (9).

$$P_{p,q}^k(n) = \begin{cases} \frac{\tau_{p,q}^\alpha(n) \cdot \eta_{p,q}^\beta(n)}{\sum_k \tau_{p,k}^\alpha(n) \cdot \eta_{p,k}^\beta(n)} & q \in M \\ 0 & \text{otherwise} \end{cases} \quad (9)$$

where n is the iterative step, M is the next city accepted of ant K and $\tau_{p,q}$ is the number of pheromones deposited during the transition from city p to q . The distance between the current city and the next city is $l_{p,q}$, $\eta_{p,q} = 1/l_{p,q}$. α and β are the parameters which control the influence of $\tau_{p,q}$ and $\eta_{p,q}$, respectively ($\alpha \geq 0, \beta \geq 1$).

After completing the n th computation cycle, the ant colony will update the $(n+1)$ th trajectory using Equations (10) and (11).

$$\tau_{p,q}(n+1) = \rho \cdot \tau_{p,q}(n) + \Delta\tau_{p,q} \quad (10)$$

$$\Delta\tau_{p,q} = \sum_{k=1}^M \Delta\tau_{p,q}^k \quad (11)$$

The ant colony from the n th stage to the $(n+1)$ th on side (p,q) is symbolised by $\Delta\tau_{p,q}$, and ant k from the n th stage to the $(n+1)$ th on side (p,q) is symbolised by $\Delta\tau_{p,q}^k$. ρ represents the pheromone evaporation coefficient, taking $0 \leq \rho \leq 1$. $\Delta\tau_{p,q}^k$ is shown in Equation (12).

$$\Delta\tau_{p,q}^k = Q/L_k \quad (12)$$

where Q is a constant and L_k is the cost of the k th ant's tour in the iterative process. The optimised parameters Q, α, β and ρ in the ACO algorithm are defined from the experiments.

Once the fitness $\Delta\lambda(n)$ becomes minimum, the optimum threshold is calculated as $\lambda(n) = \lambda(n-1) + \Delta\lambda(n)$.

The general procedure of the ACOW method is shown in Figure 4. The parameters of the ACOW algorithm are set as follows:

- (1) Number of ant colonies K is 40,
- (2) The city number M is 50,
- (3) The maximum iteration number n_{max} is 500.

4 | DENOISING EXPERIMENTS

For verifying the effectiveness of the ACOW method on signal denoising, the other three denoising methods were used to perform the denoising experiments in this article:

- (a) SW: soft wavelet method presented in [18].
- (b) GW: gradient-based wavelet method presented in [19].

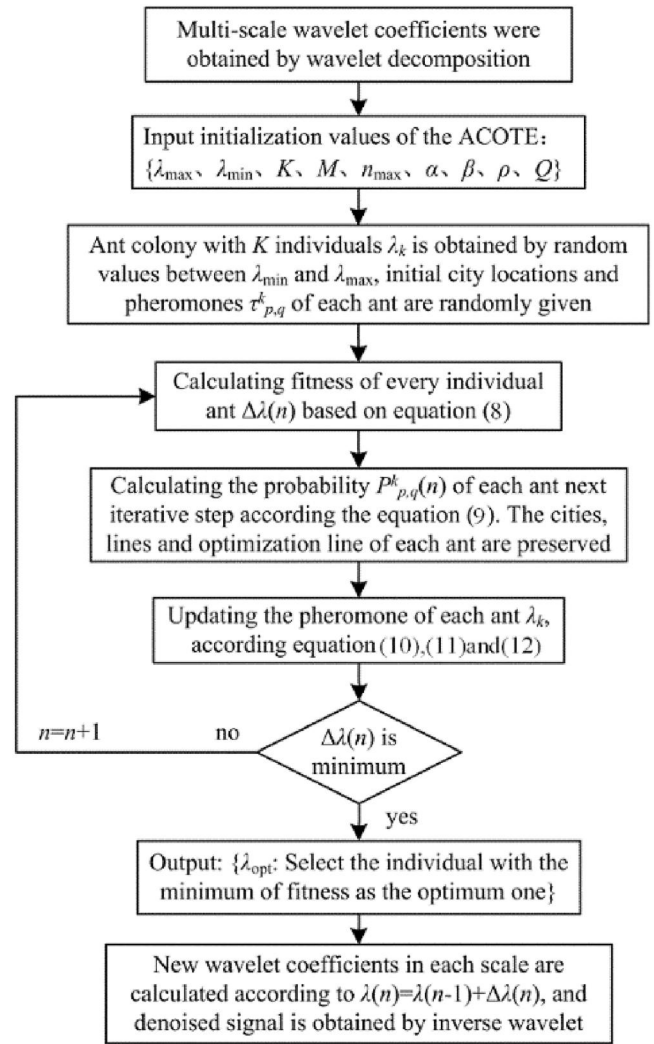


FIGURE 4 Flowchart of ant colony optimisation wavelet denoising method

- (c) GOW: genetic optimisation wavelet method presented in [17].

White noise with different signal-to-noise ratios (SNR) was embedded in different signals. And the signals embedded in white noise were denoised by the ACOW, SW, GW and GOW methods. The effectiveness of these four denoise methods was compared.

The denoising object and the denoising method have been introduced above. Next, we will compare and analyse the denoising results of using the SW, GW, GOW and ACOW denoising methods for different signals.

4.1 | Denoising of artificial signals

Four denoising methods are used to denoise artificial signals.

Figures 5–8 show the denoising results of artificial signals using four methods. The Db8 wavelet was selected in this article, and 6 was selected as the largest wavelet decomposition

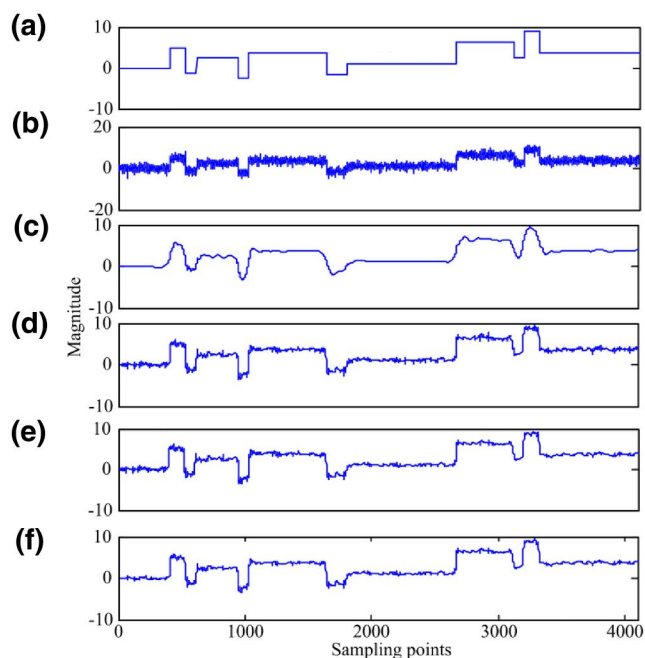


FIGURE 5 The denoised result of blocks. (a) Initial signal; (b) Initial signal with white noise; (c–f) denoised by soft wavelet, gradient-based wavelet, genetic optimisation wavelet and ant colony optimisation wavelet

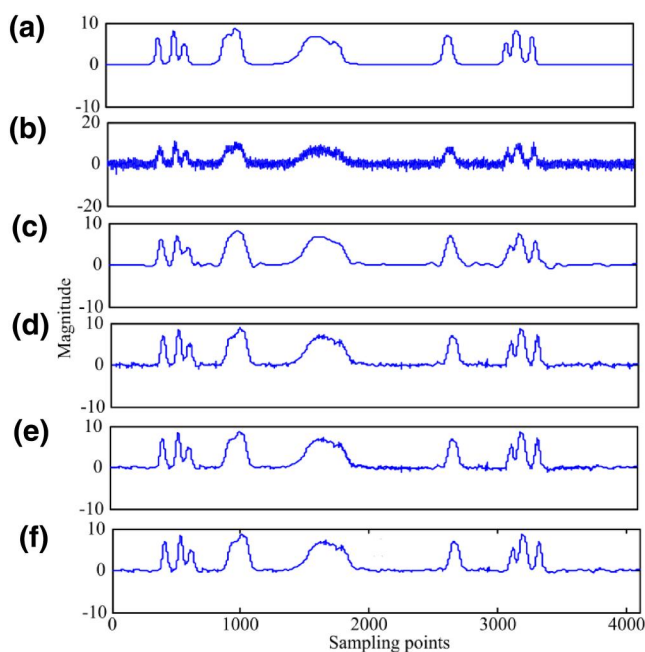


FIGURE 6 The denoised result of Bump. (a) Initial signal; (b) Initial signal with white noise; (c–f) denoised by soft wavelet, gradient-based wavelet, genetic optimisation wavelet and ant colony optimisation wavelet

level. Figure 5–8(a) are the initial signals of Blocks, Bumps, HeaviSine and Doppler. Figures 5–8(b) are the initial signals with the white noise of Blocks, Bumps, HeaviSine and

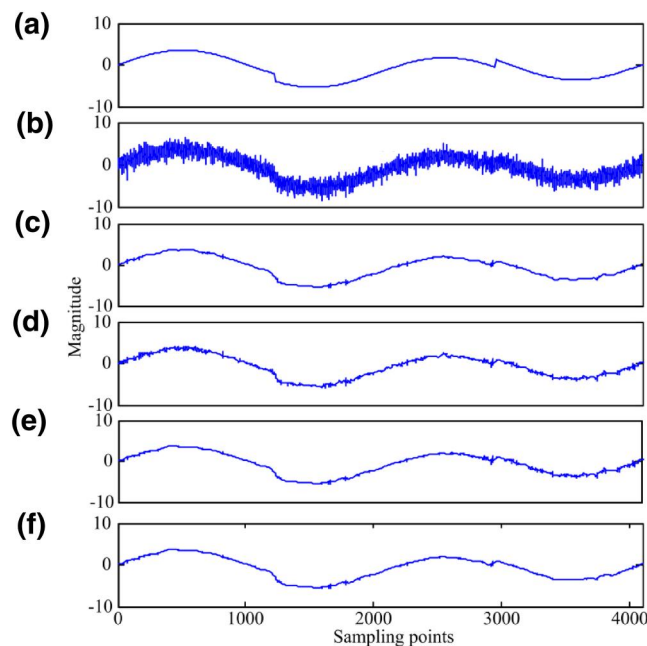


FIGURE 7 The denoised result of HeaviSine. (a) Initial signal; (b) Initial signal with white noise. (c–f) denoised by soft wavelet, gradient-based wavelet, genetic optimisation wavelet and ant colony optimisation wavelet

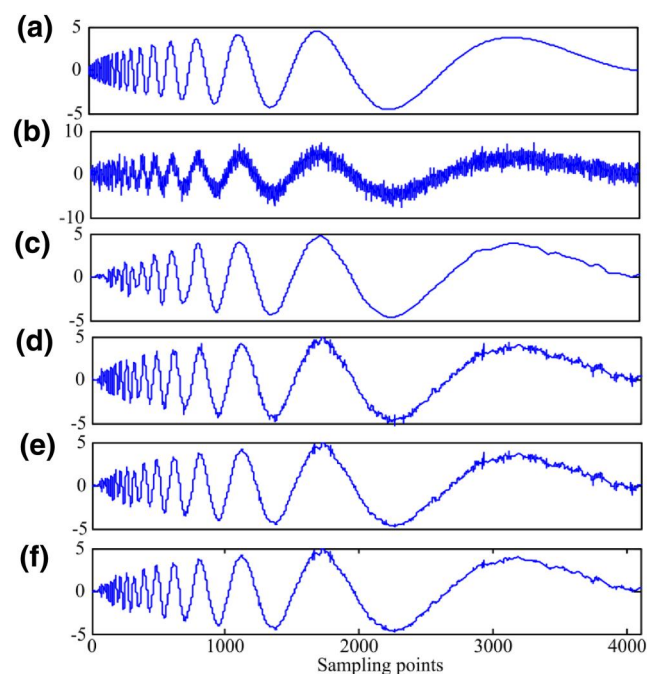


FIGURE 8 The denoised result of Doppler. (a) Initial signal; (b) Initial signal embedded in white noise. (c–f) denoised by soft wavelet, gradient-based wavelet, genetic optimisation wavelet and ant colony optimisation wavelet

Doppler. White noise with σ_s/σ_e of six is embedded in four artificially stable signals, where σ_s represents the standard deviation of the signal and σ_e represents the standard deviation of

the noise. Figure 5–8(c–e) show the denoising results of the four artificially stable signals using the SW, GW, GOW and ACOW methods, respectively. The results show that the denoising ability of the ACOW method is significantly higher than that of the other three methods. The signals after denoising are closest to the initial signals and retain more signal characteristics. In addition, it is difficult for the SW method to extract the original signals. The GW and GOW methods can retain the signal characteristics, but there is still more white noise in the four signals.

The MSE and the time cost are the criteria for measuring the effectiveness of signal denoising. Table 1 shows the (MSE) [19] of the four artificial signals using the four methods. For the same signal, the ACOW method has the minimum MSE among the four methods, followed by the GOW, GW and SW methods. It indicates that the ACOW method generates significantly smaller distortion than the other methods.

TABLE 1 Mean square errors of the four signals denoised by the four methods

Signals	Blocks	Bumps	HeaviSine	Doppler
Initial	1.0449	1.0449	1.0449	1.0449
Soft wavelet	0.3014	0.1808	0.0288	0.0923
Gradient-based wavelet	0.1228	0.0587	0.0497	0.0686
Genetic optimisation wavelet	0.1192	0.0470	0.0268	0.0507
Ant colony optimisation wavelet	0.1011	0.0450	0.0156	0.0358

TABLE 2 Time cost of the four methods (unit: second)

Signals	Methods			
	Soft wavelet	Gradient-based wavelet	Genetic optimisation wavelet	Ant colony optimisation wavelet
Blocks	0.031	140.281	8.203	1.582
Bumps	0.032	168.782	8.687	1.603
HeaviSine	0.031	150.796	8.109	1.556
Doppler	0.031	146.531	8.156	1.568

TABLE 3 The denoising result of partial discharge (PD) signals

Signals	SNR	Soft wavelet		Gradient-based wavelet		Genetic optimisation wavelet		Ant colony optimisation wavelet	
		Mean square error (MSE)	Magnitude error (ME) (%)	MSE	ME (%)	MSE	ME (%)	MSE	ME (%)
Pulse PD	1	0.0276	36.33	0.0189	25.20	0.0101	4.46	0.0065	4.27
	2	0.0113	14.78	0.0112	17.71	0.0042	4.21	0.0031	4.19
	3	0.0075	12.02	0.0066	7.41	0.0021	4.11	0.0018	3.68
	4	0.0033	8.91	0.0052	8.82	0.0016	3.65	0.0015	2.35
Vibrating PD	1	0.0246	39.76	0.0196	33.95	0.0065	17.75	0.0053	16.76
	2	0.0121	26.22	0.0111	27.06	0.0024	12.41	0.0020	11.86
	3	0.0065	19.21	0.0096	25.12	0.0015	8.22	0.0015	7.98
	4	0.0036	16.11	0.0090	22.12	0.0012	7.56	0.0010	7.22

Table 2 shows the time costs of the four methods. The SW method takes the shortest time, and the time costs of the GOW and ACOW methods are much less than that of the GW method. Furthermore, the time cost of the ACOW method amounts to only about 20 percent of that of the GOW method.

4.2 | Denoising of PD signals

The literature [21] reports that the GW method is not competent enough to denoise PD signals. Therefore, this article conducts further research on denoising PD signals with different white noise-embedded SNRs. Table 3 shows the MSE and ME of the pulse PD and vibrating PD signals [23]. After denoising the signals embedded with the same SNR by four kinds of methods, the minimum MSE and ME were obtained by the ACOW method. When the SNR is 1, the ME of the SW and GW methods exceeds 20%, while the ME of the GOW and ACOW methods is only around 4%. The MSE of the GOW method is very small at 0.0101, but the ACOW method's MSE is even smaller at 0.0065. It indicates that the GOW and ACOW methods, especially the latter one, generate smaller distortions than the SW and GW methods. Interestingly, for the same signals and denoising method, the higher the SNR, the lower the MSE and ME after denoising, which indicates that the higher the SNR, the more effectively the noise that can be captured and removed.

Table 4 shows the time cost of the four denoising methods for PD signals with an SNR of 1. The time cost of denoising PD signals by the GW method is an order of several hundreds of seconds. The time cost of the GOW method is about 3s. The time cost of the ACOW and SW methods is no more than 1s. Even the time cost of the SW method is about 0.5s less than that of the ACOW method. But the ACOW method has demonstrated superior noise removal capabilities on the MSE and ME. It shows that the ACOW method is the most effective of the four methods for denoising PD signals.

The wavelet base and the largest wavelet decomposition level used for denoising the simulative PD signals are identical to those used for denoising stable signals. Figure 9–10 show

TABLE 4 Time cost of four methods (unit: second)

Signals	Methods			
	Soft wavelet	Gradient-based wavelet	Genetic optimisation wavelet	Ant colony optimisation wavelet
Pulse partial discharge (PD)	0.078	680.046	3.016	0.592
Vibrating PD	0.062	715.134	3.891	0.618

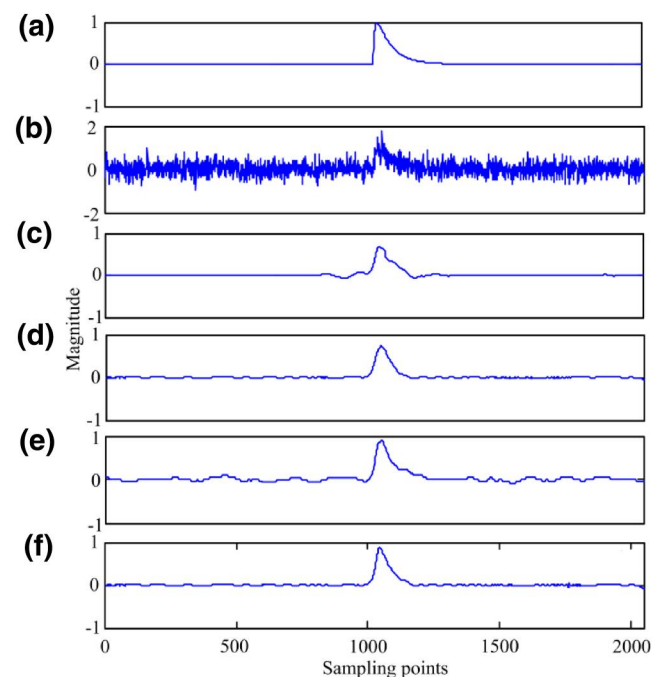


FIGURE 9 Denoised results of pulse partial discharge signal. (a) Initial signal. (b) Initial signal with simulative white noises. (c–f) Signals denoised by soft wavelet, gradient-based wavelet, genetic optimisation wavelet and ant colony optimisation wavelet

the results of four denoising methods for two different PD signals.

Figures 9–10(a) depict the initial signals of the pulse PD signal and the vibrating PD signal. Figures 9–10(b) depict the initial signals embedded with white noise, with an SNR of 1. Figures 9–10(c–e) show the denoising results of the four artificially stable signals, denoised by the SW, GW, GOW and ACOW methods. Obviously, in both PD signals, the PD signals for which the ACOW denoising method is followed are closer to the initial PD signals than those signals for which the SW, GW, and GOW methods are followed. Besides, the PD signals denoised by the ACOW methods reach the minimum ME among the four methods.

4.3 | Denoising of field-detected PD signals

The db8 wavelet was used for denoising field-detected PD signals. Figure 11 displays the signals denoised by the SW, GOW and ACOW method. The GW method is excluded because

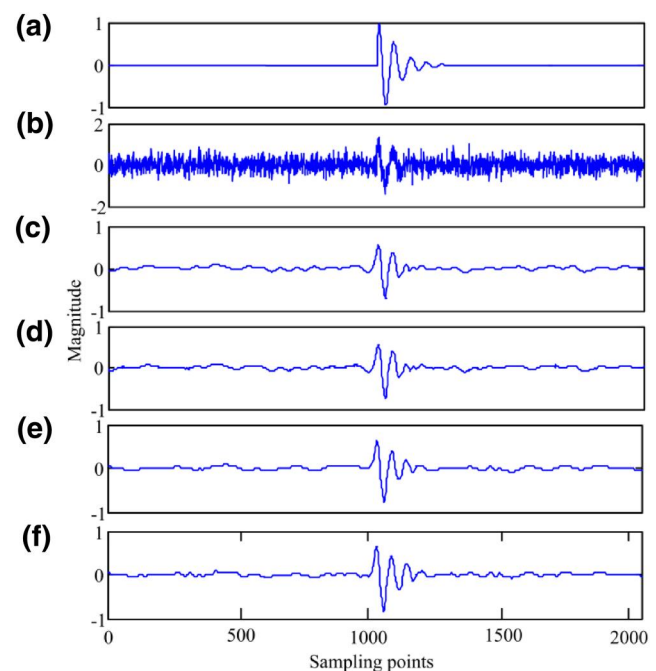


FIGURE 10 Denoised results of vibrating partial discharge signal. (a) Initial signal; (b) Initial signal embedded in simulative white noises; (c) Denoised by soft wavelet, gradient-based wavelet, genetic optimisation wavelet and ant colony optimisation wavelet

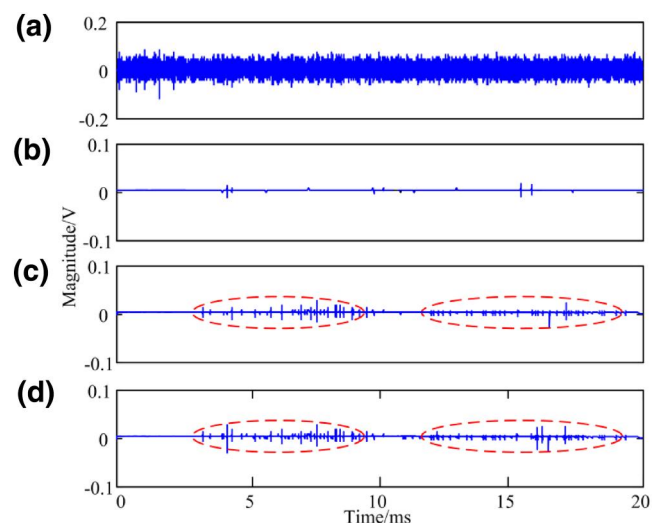


FIGURE 11 Denoising example of field partial discharge signal in a 220 kV transformer. (a) Field-detected signal; (b–d) Denoised signals by the soft wavelet, genetic optimisation wavelet and ant colony optimisation wavelet

the result of the GW method is invalid and the convergence is very slow. Figure 11(a) depicts the initial signals of the field PD signal. Figure 11(b–d) show the denoising results of the SW, GOW and ACOW methods. Figure 11(a) shows that the SW method can hardly extract PD pulses. Figures 11(c) and (d) indicate that PD pulses hidden in the noise appear, especially those pulses denoised by the ACOW method, which is focussed on by the ellipsoids. In addition, ACOW method takes less time than the GOW method. This demonstrates that the ACOW method is more competent than the SW, GW and GOW methods at denoising field-detected PD signals.

5 CONCLUSIONS

An enhanced wavelet method improved by the ACO algorithm is applied to denoise condition signals of intelligent substations. Artificial signals, simulative PD and field-detected PD signals have been used as experimental signals. The proposed ACOW, SW, GW and GOW methods are applied to denoise the selected signals. The conclusions were drawn as follows:

- (1) The denoise analysis of artificial signals shows that the signals are closest to the initial signals after denoising and retain more signal characteristics. The time cost of the ACOW method can be also shortened to a great extent.
- (2) The denoise analysis of simulative PD signals indicate that the ACOW method has a higher ability of denoising than those the SW, GW, and GOW methods. In addition, the ACOW method has less time cost than the GOW method. This indicates that the way of ACOW is a promising technique to denoise signals of electrical equipment in practical circumstance.
- (3) The denoise analysis of field-detected PD signals with strong background noise shows that the GW method can no longer converge, while the ACOW method can effectively extract weak local discharge pulses. It is shown that the ACOW method has a good denoise effect in the application of state signal processing, and it is beneficial to realising the fast and real-time network communication of intelligent substations.

Although the proposed ACOW method can effectively solve the problem of denoising compared with the AW, GW and GOW methods, it has problems such as complex calculation. Experimental results show that the time cost of the ACOW and SW methods is no more than 1s. Even the time cost of the SW method is about 0.5s less than that of the ACOW method. It indicates that the calculation speed of the ACOW method should be improved. But the ACOW method exhibited excellent results when it was adopted for signal denoising, according to the MSE and ME. The authors intend to apply the proposed technique to more complex signals, such as the EEG signal, in future studies.

ACKNOWLEDGEMENTS

This work is supported by the National Key Research and Development Program (2018YFB2100100) and the Joint Funds of the National Natural Science Foundation of China (U1866603). The project is supported by the Scientific and Technological Research Program of Chongqing Municipal Education Commission (Grant No. KJQN202001146) and the Program of Chongqing Banan District (2020QC407).

ORCID

Xiao Yang  <https://orcid.org/0000-0001-6987-9357>

Yuan Yang  <https://orcid.org/0000-0002-8111-1460>

REFERENCES

1. Mazur, D.C., et al.: Developing protective relay faceplates, taking advantage of the benefits of IEC 61850. *IEEE Ind. Appl. Mag.* 21, 33–40 (2015)
2. Aarti, E., Kaur, P.: An efficient algorithm to enhance the digital/medical image using SWT and AMF in wavelet transformation domain. In: *International Conference on Computing for Sustainable Global Development IEEE*, New Delhi (2016)
3. Martins, C.H.R., et al.: Tool condition monitoring of single-point dresser using acoustic emission and neural networks models. *IEEE Trans. Instrum. Meas.* 63, 667–679 (2014)
4. Trung, T.T., et al.: Real-time wavelet-based coordinated control of hybrid energy storage systems for denoising and flattening wind power output. *Energies*. 7, 6620–6644 (2014)
5. Tang, H., et al.: Electro-thermal comprehensive analysis method for defective bushings in HVDC converter transformer valve-side under multiple-frequency voltage and current harmonics. *Int. J. Electr. Power Energy Syst.* 130.8, 106777 (2021)
6. Zhu, Q., Cui, E.: Study of wavelet thresholding image de-noising algorithm based on improvement thresholding function. *International Conference on Computer, Networks and Communication Engineering*, Beijing (2013)
7. Prashar, N., Sood, M., Jain, S.: Dual-tree complex wavelet transform technique-based optimal threshold tuning system to deliver denoised ECG signal. *Transactions of the Institute of Measurement and Control* (2020)
8. Alyasseri, Zaa, et al.: Hybridizing β -hill climbing with wavelet transform for denoising ECG signals. *Inf. Sci.* 429, 229–246 (2017)
9. Alyasseri, Z.A.A., et al.: EEG signals denoising using optimal wavelet transform hybridized with efficient metaheuristic methods. *IEEE Access*. 8, 10584–10605 (2020)
10. Alyasseri, Zaa, et al.: ECG signal denoising using β -hill climbing algorithm and wavelet transform. In: *2017 8th International Conference on Information Technology (ICIT)*. IEEE, Amman (2017)
11. Alyasseri, Zaa, Khader, A.T., Al-Betar, M.A.: Optimal electroencephalogram signals denoising using hybrid β -Hill climbing algorithm and wavelet transform. In: *ICISPC 2017 International Conference on Imaging, Signal Processing and Communication ACM*, Penang (2017)
12. Alyasseri, Z.A.A. et al.: EEG signal denoising using hybridizing method between wavelet transform with genetic algorithm. In: Z. Md Zain, et al. (eds.), *Proceedings of the 11th National Technical Seminar on Unmanned System Technology 2019*. Lecture Notes in Electrical Engineering, vol 666. Springer, Singapore (2021)
13. A Alyasseri, Z.A., T Khader, A., Al-Betar, M.A.: Electroencephalogram signals denoising using various mother wavelet functions: a comparative analysis. In: *Proceedings of the international Conference on imaging, signal processing and communication (ICISPC 2017)*, pp. 100–105. Association for Computing Machinery, New York, 2017
14. Cai, X., et al.: An improved quantum-inspired cooperative co-evolution algorithm with multi-strategy and its application. *Expert Syst. Appl.* 171, 114629 (2021)

15. Deng, W., et al.: An improved differential evolution algorithm and its application in optimization problem. *Soft Comput.* 25, 5277–5298 (2021)
16. Wu, D.: Differential evolution algorithm with wavelet basis function and optimal mutation strategy for complex optimization problem. *Applied Soft Computing.* 100, 106724–106740 (2020)
17. Song, Y., et al.: Enhanced success history adaptive DE for parameter optimization of photovoltaic models. *Complexity.* 2021, 22 (2021)
18. Deng, W.: A novel gate resource allocation method using improved PSO-based QEA. *IEEE Trans. Intell. Transport. Syst.* 21, 10 (2020)
19. Deng, W., et al.: An enhanced MSIQDE algorithm with novel multiple strategies for global optimization problems. *IEEE Trans. Syst. Man Cybern. Syst.* 50, 1–10 (2020). <https://doi.org/10.1109/TSMC.2020.3030792>
20. Donoho, D.L., Johnstone, I.M.: Adapting to unknown smoothness via wavelet shrinkage. *J. Am. Stat. Assoc.* 90, 1200–1224 (1995)
21. Li, J., Sun, C., Yang, J.: Adaptive de-noising for PD online monitoring based on wavelet transform. *IEEE Southeast Conf.*, pp. 71–74. Memphis, 2006
22. Grefenstette, J.J.: Optimization of control parameters for genetic algorithms. *IEEE Tran. Syst. Man Cybern.* 16, 122–128 (1986)
23. Li, J. et al.: cWavelet de-noising of partial discharge signals based on genetic adaptive threshold estimation. *IEEE Trans. Dielectr. Electr. Insul.* 19, 543–549 (2012)
24. Dorigo, M., Stützle, T.: The ant colony optimization metaheuristic, pp. 25–64. cMIT Press., US (2004)
25. Nasri, M., Nezamabadi-pour, H.: Image denoising in the wavelet domain using a new adaptive thresholding function. *Neurocomputing.* 72, 1012–1025 (2009)
26. Hongyu, L., et al.: Extraction of condition signals of electrical plants by ACO wavelet threshold estimation. *Trans. China Electrotech. Soc.* 30(12), 422–428 (2015)
27. Zhao, D.H., et al.: Research of filtering based on wavelet de-noising method for revolution-modulation north-finder. *Adv. Magn. Reson.* 121–122, 934–939 (2010)
28. Chao-Hua, D., Yun-Fang, Z., Wei-Rong, C.: A novel thresholding algorithm of wavelet de-noising. *Modular machine tool & automatic manufacturing technique.* Design and Research (2005)
29. Carrera, A., Koehler, S., Rohmer, G.: Signal processor and method for processing a receiving signal. *Blood.* 105(9), 3699–706 (2005)
30. Abbate, A., et al.: Signal detection and noise suppression using a wavelet transform signal processor: application to ultrasonic flaw detection. *IEE Trans. Ultrason. Ferr. Freq. Contr.* 44(1), 14–26 (1997)
31. Z0hang, X.P., Desai, M.D.: Adaptive denoising based on SURE risk. *IEEE Signal Process. Lett.* 5(10), 265–26 (2002)

How to cite this article: Jiang, T., et al.: Wavelet method optimised by ant colony algorithm used for extracting stable and unstable signals in intelligent substations. *CAAI Trans. Intell. Technol.* 7(2), 292–300 (2022). <https://doi.org/10.1049/cit2.12054>